Check for updates

Advanced Quantum Technologies

ADVANCED QUANTUM TECHNOLOGIES
www.advquantumtech.com

RESEARCH ARTICLE

Generation of Picosecond Pulsed Bright Squeezed Light With Perfect Vortex Distribution

Jun Liu[1] | Yan Liu[1] | Xiaowei Wu[1] | Xiaolong Su[1,2]

[1]State Key Laboratory of Quantum Optics Technologies and Devices, Institute of Opto-Electronics, Shanxi University, Taiyuan, China | [2]Collaborative Innovation Center of Extreme Optics, Shanxi University, Taiyuan, Shanxi, China

Correspondence: Xiaolong Su (suxl@sxu.edu.cn)

Received: 25 January 2026 | **Revised:** 17 April 2026 | **Accepted:** 21 May 2026

Keywords: bright squeezed light | perfect vortex beam | picosecond pulse

ABSTRACT

Broadband bright squeezed states are important quantum resources that play a crucial role in quantum information and quantum measurement. Here, we present the broadband bright pulsed squeezed states generated by a single-pass optical parametric amplification based on a custom-poled potassium titanyl phosphate crystal. By optimizing the spatial mode of the picosecond pump beams, a bright squeezed light with 1.7 dB squeezing and output power of 5 mW is obtained. With a spatial light modulator, the spatial distribution of the bright squeezed light is shaped into perfect vortex beams with topological charges up to $l = 20$, while the squeezing level is 1.4 dB. The presented squeezed states provide essential resources for advanced quantum optics applications.

Graphical Abstract

1 | Introduction

Squeezed states are a vital quantum resource with widespread applications in quantum communication [1–6], quantum metrology [7–9], and quantum sensing [10–12]. Since the quadrature noise of squeezed state below the standard quantum limit (SNL), it has been used in gravitational wave detection [13–16] and optical imaging [17–19], significantly enhancing the sensitivity of these systems. A widely used approach to generate squeezed state is the optical parametric oscillators, which effectively enhances the nonlinear interaction in cavity [20–22]. By precisely controlling optical cavity losses and phase stabilization, squeezing levels up to 15 dB have been achieved [23]. However, the relatively low power of the squeezed vacuum state limits its applications in wider fields, including the quantum-enhanced interferometer and quantum-enhanced stimulated Raman scatter microscopy [24, 25], where higher squeezed light power helps improve sensitivity. To meet the increasing requirements of advanced quantum technologies, it is essential to prepare squeezed states that offer strong optical power.

Bright squeezed light with a coherent amplitude can be obtained by injecting a seed beam into an optical cavity, a process referred to as optical parametric amplification (OPA). In this way, the bright squeezed light has been demonstrated in a continuous-wave system [26, 27]. Another approach to prepare bright squeezed light is to couple a squeezed vacuum state with a strong coherent state on a low-reflectivity beam splitter. This coherently coupled scheme has been experimentally implemented to generate bright squeezed light with output power exceeding 1.3 mW and squeezing levels of 3.6 dB [24]. However, these methods rely on cavity-based continuous-wave systems, in which the achievable squeezing bandwidth is limited to tens to hundreds of MHz. By using the pulsed light, the squeezed states with broad bandwidth and high power can be prepared.

With high peak powers and ultrashort durations, pulsed lasers enable efficient nonlinear interactions in a single-pass configuration without optical cavities [28–31]. Under such conditions, the squeezing bandwidth is determined primarily by the phase-matching bandwidth of the crystal and can extend to several

© 2026 Wiley-VCH GmbH

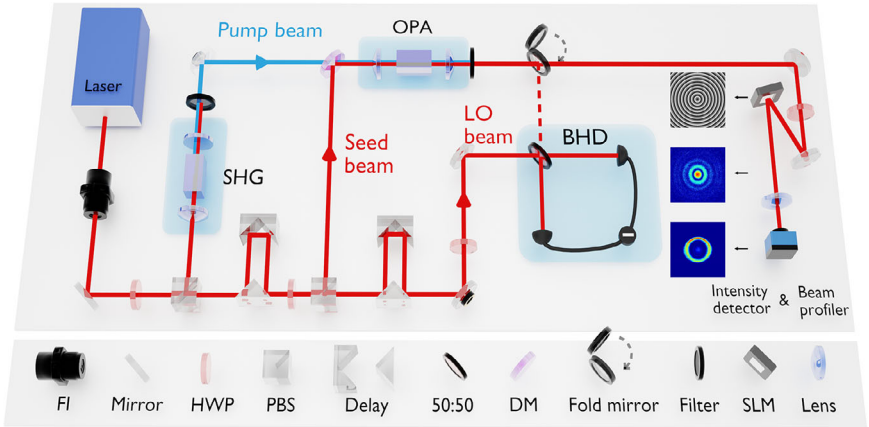

FIGURE 1 | Experimental setup. The squeezed state is generated via a single-pass OPA. By adjusting the fold mirror, either the squeezed vacuum state or the bright squeezed light can be detected. An SLM is applied to generate PV beams. The inserted figures from top to bottom show the phase diagram loaded onto the SLM, the generated Bessel–Gaussian beam, and the resulting PV beam, respectively. FI, Faraday isolator; HWP, half-wave plate; PBS, polarization beam splitter; DM, dichroic mirror; SLM, spatial light modulator; BHD, balanced homodyne detector.

hundred gigahertz. Such broadband pulsed squeezed states can serve as valuable resources for time-domain multiplexing quantum information processing [32] and can enhance imaging sensitivity in advanced imaging modalities such as pump–probe microscopy and stimulated Raman scattering microscopy [24, 25, 33–35]. Thus, it is essential to efficiently generate bright and broadband pulsed squeezed light.

Perfect vortex (PV) beams are a special class of vortex beams whose ring radius is independent of the topological charge [36–38]. This invariant spatial distribution offers advantages for mode multiplexing in free space and fiber, making PV beams particularly valuable for optical communication applications and information processing [39–41]. At present, various methods have been developed to generate classical PV beams [42–44]. However, research on squeezed light in PV modes remains relatively limited [45, 46].

In this letter, we observe a 3 dB squeezed vacuum state in a single-pass OPA with a bandwidth over 100 MHz. With the injection of a seed beam, we demonstrate a broadband pulsed bright-amplitude-squeezed state with 1.7 dB of noise reduction below SNL and an output power of 5 mW. By shaping the bright pulsed squeezed light using a spatial light modulator (SLM), we generate squeezed light with a PV distribution. We observe 1.4 dB squeezing for the PV beam with topological charges of 20. This work provides an essential resource for high-dimensional quantum information processing and high-sensitivity quantum imaging.

2 | Experimental Setup

As shown in Figure 1, a pulsed laser (APE, picoEmerald S) with a repetition rate of 80 MHz and pulse duration of 2 ps at 1031.3 nm is employed as a laser source. To protect the laser from back reflections, an optical Faraday isolator is placed after the laser output. With the combination of a half-wave plate and a polarizing beam splitter (PBS), the laser beam is split into two portions; one serves as the fundamental wave for the second-harmonic generation (SHG) process, while the other is utilized as the seed beam for the OPA process. Benefiting from the high peak power of the pulsed laser, high-performance SHG with a maximum conversion efficiency of 29.1% is achieved in a 2 mm custom-poled $KTiOPO_4$ (CPKTP) crystal, allowing for an output power of 350 mW [47]. This second-harmonic wave is then employed as the pump source of the OPA process.

The second harmonic and seed beam are combined via a dichroic mirror (Semrock, NFD01-1040) and then simultaneously focused into the OPA. To ensure temporal overlap of the two pulses, a delay line is used to synchronize their arrival times. The OPA consists of a type-0 phase-matched CPKTP crystal with dimensions of $1 \times 2 \times 5$ mm^3, whose 1×2 mm^2 facets are anti-reflection coated at 1031.3 and 515.7 nm. For precise temperature control, the crystal is mounted in a custom-built oven. Its temperature is actively stabilized with a temperature controller, maintaining fluctuations below 0.1 °C. After the squeezed state is prepared, the residual pump light is blocked by a filter (Semrock, FF01-1001). To characterize the squeezing levels of both the pulsed squeezed vacuum state and the bright squeezed light, a balanced homodyne detector (BHD) and an intensity detector are employed, respectively. A fold mirror is inserted to enable flexible switching between the two detection paths. We generate a bright squeezed light with Bessel–Gaussian (BG) distribution by loading the phase diagram of a BG beam onto an SLM first, and then obtain the corresponding PV beam by performing a Fourier transform with a lens [38, 48]. The intensity distribution of the PV beam is recorded with a beam profiler, and its squeezing level is characterized using an intensity detector.

3 | Results

3.1 | Picosecond Pulsed Squeezed Vacuum State

The bright squeezed light can be regarded as a coherent displacement of the corresponding vacuum-squeezed state in phase space. Therefore, achieving strong vacuum squeezing is essential for obtaining high-quality bright squeezing. Moreover, establishing a well-optimized squeezed vacuum state also enables precise

25119044, 2026, 6, Downloaded from https://advanced.onlinelibrary.wiley.com/doi/10.1002/qute.70334 by Shanxi University, Wiley Online Library on [16/06/2026]. See the Terms and Conditions (https://onlinelibrary.wiley.com/terms-and-conditions) on Wiley Online Library for rules of use; OA articles are governed by the applicable Creative Commons License

calibration of the parametric gain, phase matching, and detection efficiency of the system.

The pulsed squeezed vacuum state is generated when the pump beam passes through the OPA without the seed beam. To enhance the nonlinear interaction and achieve optimal squeezing, the pump beam waist at the center of the crystal is adjusted such that the Boya–Kleinman focusing parameter $\xi = L/b$ equals unity [49]. Here, L is the crystal length and $b = 2\pi\omega_0^2 n/\lambda$ is the confocal parameter, where n is the refractive index of the crystal at the wavelength of λ. Besides the pump beam size, the pump power and detection efficiency also affect the squeezing level, which is expressed as

$$S_{\pm} = \eta \exp(\pm 2r) + 1 - \eta, \tag{1}$$

where S_+ and S_- represent the anti-squeezed and squeezed level, respectively, η denotes the overall efficiency, and $r = c\sqrt{p}$ is the squeezing parameter with p the pump power [28, 29]. In this system, we have an interference visibility of 0.93, corresponding to interference efficiency η_v of 0.86, an average photodiode (Fermionics, FD100) quantum efficiency η_{QE} of 0.86, and an optical transmission efficiency η_t of 0.95. The electronic noise of the BHD also contributes to the degradation of the total efficiency. For a given SNR, the corresponding measurement efficiency is given by $\eta_{SNR} = \frac{SNR-1}{SNR}$ [50]. Accounting for all loss contributions, the overall detection efficiency $\eta = \eta_v \cdot \eta_{QE} \cdot \eta_t \cdot \eta_{SNR} = 0.64$.

After optimizing the beam size and detection efficiency, we measure the picosecond-pulsed squeezed vacuum state at 20 MHz, as shown in Figure 2a. A maximum noise suppression of 3 dB below the SNL is observed. Figure 2b presents the broadband noise spectrum of the picosecond-pulsed squeezed vacuum state. Limited by the detector bandwidth, quantum noise suppression is only observed in the 0–100 MHz range. The theoretical bandwidth of the squeezed state generated in a single-pass configuration can reach several hundred gigahertz, affected by the phase-matching linewidth of the nonlinear crystal [30]. By using higher-bandwidth detectors or employing an optical parametric amplification before the photo-detection, a broader bandwidth of squeezed light can be observed or utilized [51, 52]. The squeezing level gradually improves and stabilizes at 100 mW when varying the pump powers, as shown in Figure 2c. By substituting the experimentally obtained squeezing and antisqueezing levels into Equation (1), we obtain the squeezing parameter and overall detection efficiency, as shown in Figure 2d. The squeezing parameter exhibits a linear dependence on the square root of the pump power, as predicted by Equation (1). The fitted overall detection efficiency yields an average value of 0.63, in agreement with the experimental value.

Although using a photodetector with higher quantum efficiency would increase the observed squeezing level, the fundamental limits on the squeezing of the picosecond-pulsed squeezed vacuum state are determined by two primary factors. First, the nonlinear conversion efficiency of the CPKTP crystal is relatively low. Employing a waveguide can increase the power density and thus strengthen the nonlinear interaction. Second, a spatiotemporal mode mismatch between the squeezed vacuum state and the LO beam. The spatiotemporal modes of the squeezed states are altered after passing through the nonlinear crystal, preventing perfect matching with the LO beam. Using an additional crystal to shorten the pulse width of the LO beam would improve mode matching and enable the observation of higher squeezing levels.

3.2 | Picosecond-Pulsed Bright Squeezed Light

A picosecond-pulsed bright squeezed light is prepared when a seed beam is injected into the OPA. We adjust the waist of the seed beam to be $\sqrt{2}$ times that of the pump beam, so that both beams have the same confocal parameter, ensuring optimal spatial mode matching. To characterize the squeezing level of the picosecond-pulsed bright squeezed light, a resonant intensity detector is employed [25]. As shown in Figure 3a, the detector exhibits a linear response for input powers up to 5 mW. We lock the OPA to the deamplified phase, generating an amplitude–quadrature squeezed state. The squeezing level of the picosecond-pulsed bright pulsed light is determined by comparing its noise spectrum with that of the coherent beam at the same power. A noise reduction of 1.7 dB for picosecond-pulsed bright pulsed light with a power of 5 mW at 20 MHz is observed, as shown in Figure 3b. Here, the squeezed bandwidth is also limited by the detector bandwidth, as that of the squeezed vacuum state.

We also measure the squeezing levels of the bright squeezed light as a function of pump power. With the increase of pump power, the squeezing level reaches maximum at 10 mW, and then decreases with further increases of pump power, as shown in Figure 3c. The decrease in squeezing when the pump power exceeds 10 mW can be attributed to two primary factors. First, the noise of the pump beam is transferred to the squeezed light in the OPA process. Second, since the amplitude-quadrature bright squeezed light is generated in the deamplification process of OPA, when the injected seed power is held constant, the increase of the pump power leads to the decrease of the output power of the squeezed light. In this case, the output of the intensity detector for the SNL and squeezed light decreases simultaneously, which makes the effect of the electronic noise of the detector more serious and leads to the decrease of the measured squeezing level.

In our experiment, the measured squeezing level of the picosecond-pulsed bright squeezed light is lower than that of the squeezed vacuum state. This is because the seed beam is not a perfectly coherent light and carries additional technical noise of approximately 4 dB above the SNL at a sideband frequency of 20 MHz. Although higher seed power leads to increased brightness of the squeezed light, it also results in a degradation of squeezing. Therefore, it is essential to reduce the noise of the seed beam of OPA to further increase the squeezing level of picosecond-pulsed bright squeezed light.

3.3 | Pulsed Bright Squeezed Light With PV Distribution

After preparing the picosecond-pulsed bright squeezed light, we convert it into a PV beam using an SLM and record the intensity distributions using a beam profiler. As shown in Figure 4a, as the topological charge increases from $l = 0$ to $l = 5$, the ring radius of the generated beam increases by only about 5%, exhibiting the

25119044, 2026, 6, Downloaded from https://advanced.onlinelibrary.wiley.com/doi/10.1002/qute.70334 by Shanxi University, Wiley Online Library on [16/06/2026]. See the Terms and Conditions (https://onlinelibrary.wiley.com/terms-and-conditions) on Wiley Online Library for rules of use; OA articles are governed by the applicable Creative Commons License

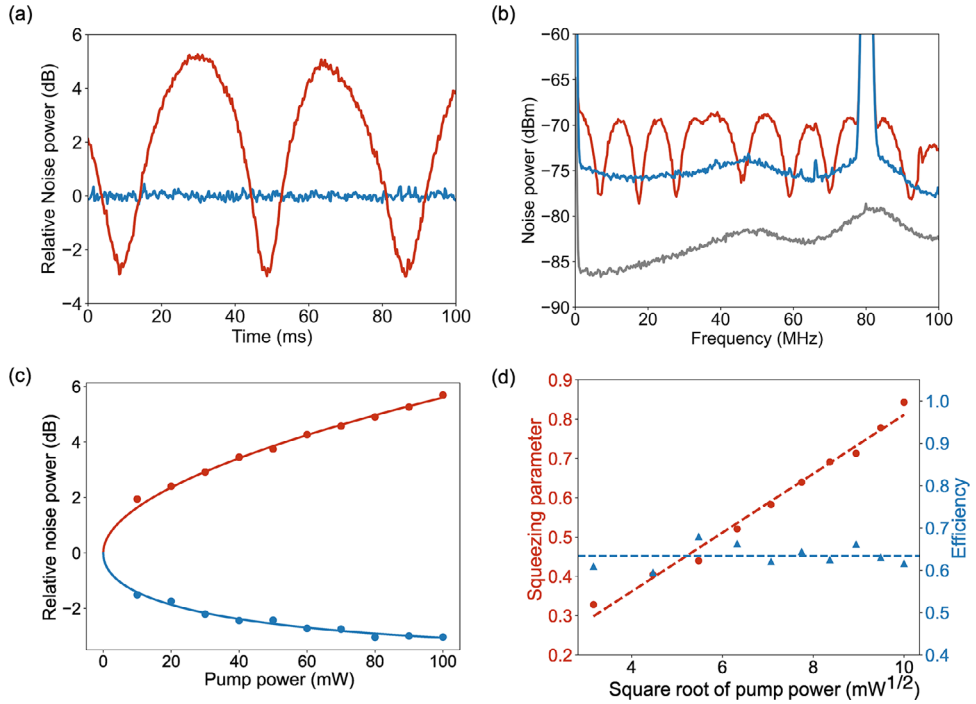

FIGURE 2 | Measurements of the picosencond-pulsed squeezed vacuum state. (a,b) Noise distribution of the picosencond-pulsed squeezed vacuum state measured at 20 and 0–100 MHz, respectively. The pump and LO power are set to 100 and 3 mW. The red trace shows the quantum noise measured during LO phase scanning using a piezoelectric transducer. The blue trace represents the SNL, obtained with the signal path blocked. The gray trace denotes the electronic noise floor of the BHD. The peak at 80 MHz corresponds to the repetition rate of the pulsed laser. RBW: 300 kHz, VBW: 100 Hz. (c) Squeezing and anti-squeezing levels of the squeezed vacuum state as a function of pump power. The blue and the red points denote the squeezed and anti-squeezed quadrature level, respectively. (d) The squeezing parameter and overall detection efficiency versus the square root of the pump average power. The red points and blue markers represent the squeezing parameter and the overall detection efficiency, respectively.

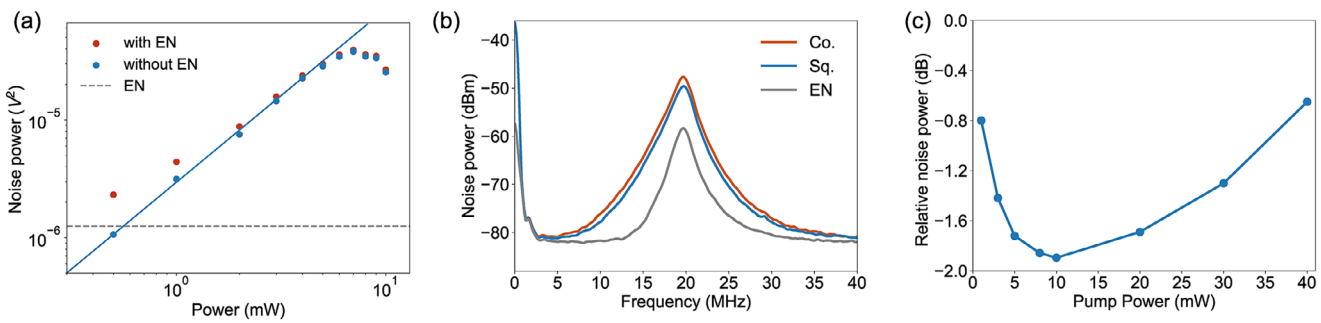

FIGURE 3 | Measurement of the picosecond-pulsed bright squeezed light. (a) Linearity characterization of the resonant intensity detector used for pulsed light. The gray trace represents the electronic noise floor of the intensity detector. This detector saturates at around 5 mW. (b) Broadband noise spectrum of bright pulsed squeezed light measured with a resonant intensity detector. The red and blue trace corresponds to the noise spectra of the 5 mW coherent beam and the bright pulsed squeezed light, respectively. (c) Squeezing level of the bright pulsed squeezed light as a function of the input pump power. The injected seed beam power is fixed at 5 mW.

characteristic of a PV beam. By interfering with a Gaussian beam, spiral interferograms are obtained, as shown in Figure 4b. The topological charge of the PV beam can be identified clearly by counting the number of spiral fringes. In this experiment, perfect vortex beams with topological charges up to $l = 20$ are observed. The maximum observable order is limited by the pixel resolution of the SLM and the spatial resolution of the CMOS camera. Moreover, zero-order diffraction leads to a gradually emerging bright spot at the beam center, causing the generated PV beam to deviate from its ideal profile.

We further characterize the squeezing levels of PV bright-pulsed squeezed states using an intensity detector. As shown in Figure 4c, the squeezing level of the zeroth-order PV beam is approximately 1.5 dB, which is lower than 1.7 dB of the unmodulated bright pulsed squeezed state. The degradation mainly arises from the increased optical losses, including four mirrors ($\eta_{\mathrm{mirror}} = 0.99$), two lenses ($\eta_{\mathrm{lens}} = 0.99$), a half-wave plate ($\eta_{\mathrm{HWP}} = 0.98$), and the SLM ($\eta_{\mathrm{SLM}} = 0.98$) itself. The total transmission loss of these elements is approximately 10%. As the topological charge of PV beams increases, we observe that the squeezing level of

25119044, 2026, 6, Downloaded from https://advanced.onlinelibrary.wiley.com/doi/10.1002/qute.70334 by Shanxi University, Wiley Online Library on [16/06/2026]. See the Terms and Conditions (https://onlinelibrary.wiley.com/terms-and-conditions) on Wiley Online Library for rules of use; OA articles are governed by the applicable Creative Commons License

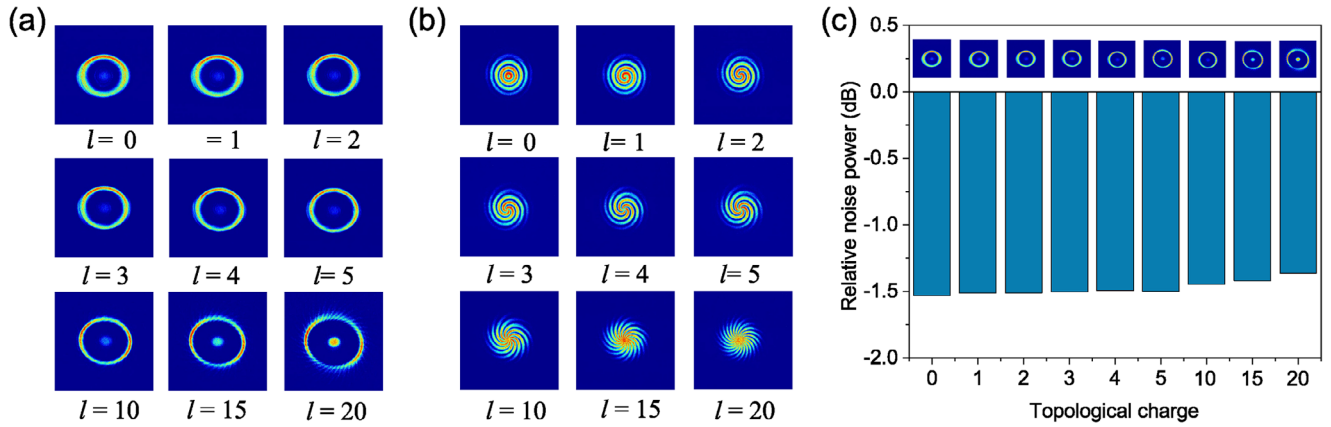

FIGURE 4 | Measurement of the picosecond-pulsed bright squeezed light with PV distribution. (a) The intensity distribution of the PV beams with topological charges from $l = 0$ to $l = 20$. (b) The corresponding interferograms of the PV beams with the Gaussian beam. (c) The squeezing levels of picosecond pulsed bright squeezed light carrying PV modes for topological charges from $l = 0$ to $l = 20$.

bright squeezed light does not change too much. When $l = 20$, the efficiency of the SLM decreases to $\eta_{SLM} = 0.93$, and a 1.4 dB noise reduction below SNL is observed. These results indicate that the observed squeezing of PV beams is insensitive to the topological charge l and is primarily related to the overall optical loss.

4 | Conclusion

In summary, we achieve both vacuum and bright pulsed squeezed states using a single-pass OPA pumped by picosecond pulses. By optimizing the spatiotemporal mode of the beams, we observe 3 dB squeezing for the picosecond pulsed squeezed vacuum state and 1.7 dB squeezing for the picosecond pulsed bright squeezed light at an output power of 5 mW. By shaping the picosecond pulsed bright squeezed light with an SLM, we generate bright squeezed light with a PV distribution, exhibiting a squeezing level of 1.4 dB at $l = 20$. Our work provides an effective approach for generating picosecond pulsed bright squeezed light with PV distribution, which has potential applications in high-dimensional quantum information processing and high-sensitivity quantum imaging.

Acknowledgements

This research was supported by the National Key Scientific Instrument and Equipment Development Projects of China (No. 2022YFF0706002), the National Natural Science Foundation of China (Grant No. U25A20525), and the Fund for Shanxi "1331 Project" Key Subjects Construction.

Conflicts of Interest

The authors declare no conflicts of interest.

Data Availability Statement

Data underlying the results presented in this paper are not publicly available at this time but may be obtained from the authors upon reasonable request.

References

1. A. Furusawa, J. L. Sørensen, S. L. Braunstein, et al., "Unconditional Quantum Teleportation," *Science* 282, no. 5389 (1998): 706–709.

2. C. Peuntinger, B. Heim, C. R. Müller, et al., "Distribution of Squeezed States Through an Atmospheric Channel," *Physical Review Letters* 113, no. 6 (2014): 060502.

3. S. L. Braunstein and P. van Loock, "Quantum Information With Continuous Variables," *Reviews of Modern Physics* 77, no. 2 (2005): 513–577.

4. F. Kaiser, B. Fedrici, A. Zavatta, et al., "A Fully Guided-Wave Squeezing Experiment for Fiber Quantum Networks," *Optica* 3, no. 4 (2016): 362–365.

5. X. Deng, S. Hao, C. Tian, et al., "Disappearance and Revival of Squeezing in Quantum Communication With Squeezed State Over a Noisy Channel," *Applied Physics Letters* 108, no. 8 (2016): 081105.

6. C. Li, S. Ren, Y. Yan, et al., "Distribution of polarization squeezed light through a 20 km fiber channel," *Science China Information Sciences* 67, no. 5 (2024): 159501.

7. G. S. Atkinson, E. J. Allen, G. Ferranti, et al., "Quantum Enhanced Precision Estimation of Transmission With Bright Squeezed Light," *Physical Review Applied* 16, no. 4 (2021): 044031.

8. Z. Tao, Y. Ren, A. Abdukirim, et al., "Phase-Sensitive Nonclassical Properties in Quantum Metrology With a Displaced Squeezed Vacuum State," *Journal of the Optical Society of America B* 38, no. 5 (2021): 1662–1668.

9. D. Adamou, L. Hirsch, T. Shields, et al., "Quantum-Enhanced Time-Domain Spectroscopy," *Science Advances* 11, no. 4 (2025): eadt2187.

10. C. L. Degen, F. Reinhard, and P. Cappellaro, "Quantum Sensing," *Reviews of Modern Physics* 89, no. 3 (2017): 035002.

11. M. Gessner, A. Smerzi, and L. Pezzè, "Multiparameter Squeezing for Optimal Quantum Enhancements in Sensor Networks," *Nature Communications* 11, no. 1 (2020): 3817.

12. B. J. Lawrie, P. D. Lett, A. M. Marino, et al., "Quantum Sensing With Squeezed Light," *ACS Photonics* 6, no. 6 (2019): 1307–1318.

13. C. M. Caves, "Quantum-Mechanical Noise in an Interferometer," *Physical Review D* 23, no. 8 (1981): 1693–1708.

14. J. Abadie, B. P. Abbott, R. Abbott, et al., "A Gravitational Wave Observatory Operating Beyond the Quantum Shot-Noise Limit," *Nature Physics* 7, no. 12 (2011): 962–965.

15. J. Aasi, J. Abadie, B. P. Abbott, et al., "Enhanced Sensitivity of the LIGO Gravitational Wave Detector by Using Squeezed States of Light," *Nature Photonics* 7, no. 8 (2013): 613–619.

25119044, 2026, 6, Downloaded from https://advanced.onlinelibrary.wiley.com/doi/10.1002/qute.70334 by Shanxi University, Wiley Online Library on [16/06/2026]. See the Terms and Conditions (https://onlinelibrary.wiley.com/terms-and-conditions) on Wiley Online Library for rules of use; OA articles are governed by the applicable Creative Commons License

16. F. Acernese, M. Agathos, L. Aiello, et al., "Increasing the Astrophysical Reach of the Advanced Virgo Detector via the Application of Squeezed Vacuum States of Light," *Physical Review Letters* 123, no. 23 (2019): 231108.

17. M. A. Taylor, J. Janousek, V. Daria, et al., "Biological Measurement Beyond the Quantum Limit," *Nature Photonics* 7, no. 3 (2013): 229–233.

18. P.-A. Moreau, E. Toninelli, T. Gregory, et al., "Imaging With Quantum States of Light," *Nature Reviews Physics* 1, no. 6 (2019): 367–380.

19. N. P. Mauranyapin, A. Terrasson, and W. P. Bowen, "Quantum Biotechnology," *Advanced Quantum Technologies* 5, no. 9 (2022): 2100139.

20. S. Suzuki, H. Yonezawa, F. Kannari, et al., "7dB Quadrature Squeezing at 860nm With Periodically Poled $KTiOPO_4$," *Applied Physics Letters* 89, no. 6 (2006): 061116.

21. Y. Takeno, M. Yukawa, H. Yonezawa, et al., "Observation of -9 dB Quadrature Squeezing With Improvement of Phase Stability in Homodyne Measurement," *Optics Express* 15, no. 7 (2007): 4321–4327.

22. H. Vahlbruch, M. Mehmet, S. Chelkowski, et al., "Observation of Squeezed Light With 10-dB Quantum-Noise Reduction," *Physical Review Letters* 100, no. 3 (2008): 033602.

23. H. Vahlbruch, M. Mehmet, K. Danzmann, and R. Schnabel, "Detection of 15 dB Squeezed States of Light and Their Application for the Absolute Calibration of Photoelectric Quantum Efficiency," *Physical Review Letters* 117, no. 11 (2016): 110801.

24. R. B. de Andrade, H. Kerdoncuff, K. Berg-Sørensen, et al., "Quantum-Enhanced Continuous-Wave Stimulated Raman Scattering Spectroscopy," *Optica* 7, no. 5 (2020): 470–475.

25. C. A. Casacio, L. S. Madsen, A. Terrasson, et al., "Quantum-Enhanced Nonlinear Microscopy," *Nature* 594, no. 7862 (2021): 201–206.

26. X. Sun, Y. Wang, L. Tian, et al., "Dependence of the Squeezing and Anti-Squeezing Factors of Bright Squeezed Light on the Seed Beam Power and Pump Beam Noise," *Optics Letters* 44, no. 7 (2019): 1789–1792.

27. Y. Tian, Y. Wang, W. Wang, et al., "Reservoir-Engineered Squeezed Lasing through the Parametric Coupling," *Physical Review Letters* 134, no. 24 (2025): 243803.

28. K. K. T. Hirano, T. Ishibashi, S. Okude, and T. Kuwamoto, "3 dB Squeezing by Single-Pass Parametric Amplification in a Periodically Poled $KTiOPO_4$ Crystal," *Optics Letters* 30, no. 13 (2005): 1722–1724.

29. Y. Eto, A. Koshio, A. Ohshiro, et al., "Efficient Homodyne Measurement of Picosecond Squeezed," *Optics Letters* 36, no. 23 (2011): 4653–4655.

30. K.-I. Yoshino, T. Aoki, and A. Furusawa, "Generation of Continuous-Wave Broadband Entangled Beams Using Periodically Poled Lithium Niobate Waveguides," *Applied Physics Letters* 90, no. 4 (2007): 041111.

31. A. Terrasson, N. P. Mauranyapin, C. A. Casacio, et al., "Fast Biological Imaging With Quantum-Enhanced Raman Microscopy," *Optics Express* 32, no. 21 (2024): 36193–36206.

32. S. Yokoyama, A. Sakaguchi, W. Asavanant, et al. "Full-Stack Analog Optical Quantum Computer with A Hundred Inputs," preprint, arXiv, June 19, 2025, arXiv:2506.16147.

33. G. Yang, C. Yang, Y. Chen, et al., "Direct Imaging of Integrated Circuits in CPU With 60 nm Super-Resolution Optical Microscope," *Nano Letters* 21, no. 9 (2021): 3887–3893.

34. C. W. Freudiger, W. Min, B. G. Saar, et al., "Label-Free Biomedical Imaging With High Sensitivity by Stimulated Raman Scattering Microscopy," *Science* 322, no. 5909 (2008): 1857–1861.

35. B. G. Saar, C. W. Freudiger, J. Reichman, et al., "Video-Rate Molecular Imaging in Vivo With Stimulated Raman Scattering," *Science* 330, no. 6009 (2010): 1368–1370.

36. S. Chen, J. Chen, T. Xia, et al., "Optical Vortices in Communication Systems: Mode (De)Modulation, Processing, and Transmission," *Advanced Photonics* 7, no. 4 (2025): 044001.

37. X. Tao, Y. Liang, S. Zhang, et al., "Generation of Perfect Vortex Beams With Complete Control Over the Ring Radius and Ring Width," *Photonics* 10, no. 12 (2023): 1382.

38. P. Vaity and L. Rusch, "Perfect Vortex Beam: Fourier Transformation of a Bessel Beam," *Optics Letters* 40, no. 4 (2015): 597–600.

39. Y. Shen, X. Wang, Z. Xie, et al., "Optical Vortices 30 Years On: OAM Manipulation From Topological Charge to Multiple Singularities," *Light: Science & Applications* 8, no. 1 (2019): 90.

40. M. Erhard, R. Fickler, M. Krenn, and A. Zeilinger, "Twisted Photons: New Quantum Perspectives in High Dimensions," *Light: Science & Applications* 7, no. 3 (2018): 146.

41. C. He, Y. Shen, and A. Forbes, "Towards Higher-Dimensional Structured Light," *Light: Science & Applications* 11, no. 1 (2022): 205.

42. H. Ahmed, H. Kim, Y. Zhang, et al., "Optical Metasurfaces for Generating and Manipulating Optical Vortex Beams," *Nanophotonics* 11, no. 5 (2022): 941–956.

43. Y. Liu, Y. Ke, J. Zhou, et al., "Generation of Perfect Vortex and Vector Beams Based on Pancharatnam-Berry Phase Elements," *Scientific Reports* 7, no. 1 (2017): 44096.

44. A. S. Ostrovsky, C. Rickenstorff-Parrao, and V. Arrizón, "Generation of the "Perfect" Optical Vortex Using a Liquid-Crystal Spatial Light Modulator," *Optics Letters* 38, no. 4 (2013): 534–536.

45. Z. Wang, Z. Zhan, A. N. Vetlugin, et al., "Structured Light Analogy of Quantum Squeezed States," *Light: Science & Applications* 13, no. 1 (2024): 297.

46. Z. Wang, Z. Shi, Y. Shen, et al., "Squeezed Coherent States of Geometric Beams," *ACS Photonics* 11, no. 10 (2024): 4407–4413.

47. Y. Zhang, J. Liu, Z. Qin, et al., "Double-Pass Second-Harmonic Generation of Picosecond Pulses With Custom-Poled KTP Crystal," *Optics Continuum* 3, no. 3 (2024): 461–467.

48. Y. Liang, S. Yan, M. He, et al., "Generation of a Double-Ring Perfect Optical Vortex by the Fourier Transform of Azimuthally Polarized Bessel Beams," *Optics Letters* 44, no. 6 (2019): 1504–1507.

49. G. D. Boyd and D. A. Kleinman, "Parametric Interaction of Focused Gaussian Light Beams," *Journal of Applied Physics* 39, no. 8 (1968): 3597–3639.

50. J. F. Tasker, J. Frazer, G. Ferranti, et al., "Silicon Photonics Interfaced With Integrated Electronics for 9 GHz Measurement of Squeezed Light," *Nature Photonics* 15, no. 1 (2021): 11–15.

51. S. Wang, X. Niu, G. Wu, and R. Dong, "1.55 GHz Balanced Homodyne Detector With High Gain Flatness Based on Low Noise Amplifier" *Review of Scientific Instruments* 96, no. 2 (2025): 023003.

52. Y. Shaked, Y. Michael, R. Z. Vered, et al., "Lifting the Bandwidth Limit of Optical Homodyne Measurement With Broadband Parametric Amplification" *Nature Communications* 9, no. 1 (2018): 609.

25119044, 2026, 6, Downloaded from https://advanced.onlinelibrary.wiley.com/doi/10.1002/qute.70334 by Shanxi University, Wiley Online Library on [16/06/2026]. See the Terms and Conditions (https://onlinelibrary.wiley.com/terms-and-conditions) on Wiley Online Library for rules of use; OA articles are governed by the applicable Creative Commons License